PROCEEDINGS, 44th Workshop on Geothermal Reservoir Engineering
Stanford University, Stanford, California, February 11-13, 2019
SGP-TR-214

Characterizing Fracture Flow in EGS Collab Experiment Based on Stochastic Modeling of Tracer Recovery

Hui Wu[1], Pengcheng Fu[1], Joseph P. Morris[1], Earl D. Mattson[2], Adam J. Hawkins[3, 4], Yuran Zhang[3], Randolph R. Settgast[1], Frederick J. Ryerson[1] and EGS Collab Team[4]

[1]Atmospheric, Earth, and Energy Division, Lawrence Livermore National Laboratory, Livermore, CA 94550

[2]Energy Recovery and Sustainability Department, Idaho National Laboratory, Idaho Falls, ID, USA.

[3]Department of Energy Resources Engineering, Stanford University, Stanford, CA, USA.

[4]TomKat Center for Sustainable Energy, Stanford University, Stanford, CA, USA.

E-mail address: wu40@llnl.gov

Keywords: enhanced geothermal systems, EGS Collab, fracture flow, tracer test, stochastic modeling

ABSTRACT

The characterization of flow behavior in fracture network is important for the optimal design and long-term management of enhanced geothermal systems (EGS). In this study, we investigate the feasibility of characterizing fracture flow patterns in the EGS Collab experiment through stochastic modeling of tracer tests. A fracture model involving connected hydraulic and natural fractures is first developed based on applicable field data, including core logs, seismic events, DTS and flow measurements. An injection well, a production well and multiple monitoring wells are also included in the model according to experiment design. We then use a brute-force, Monte Carlo approach to perform massive realizations to simulate tracer transport processes in the hydraulic and natural fractures, and tracer breakthrough curves at multiple monitoring wells are obtained for each realization. A fitting criterion is then employed to select viable solutions that yield optimal fits of the measured tracer breakthrough curves. Through these selected solutions, we estimate the aperture distributions in the hydraulic and natural fractures and try to identify flow patterns in the fracture model. The modeling study indicates that the aperture of the hydraulic fracture is about 100 microns, and the aperture of the natural fracture is about one magnitude larger. The flow field in the natural fracture might be more channelized than that in the hydraulic fracture. We also find that the fluid/tracer may leak from the hydraulic fracture to matrix through a sink to the left of the hydraulic fracture.

1. INTRODUCTION

Enhanced geothermal system (EGS) provides a promising solution for the increasing global demand of electric power (Vogt et al., 2012; Guo et al., 2016a; Lu et al., 2018). Heat resources stored in subsurface hot dry rock (HDR) is extracted by circulating fluid through injection and production wells connected by the fractur network in the HDR. One of the key factors for a successful EGS development is an enhanced permeability in the target HDR which can promote fluid flow between injection and production wells and also enlarge the effective heat exchange area. Hydraulic fracturing has been used to create fractures in low-permeability HDR to improve heat extraction efficiency in EGS (Brown et al., 2012; McClure and Horne, 2014; Cladouhos et al., 2016; Fu et al., 2016). The stimulated hydraulic fractures and pre-existed natural fractures together form a fracture network that provides main flow paths for fluid circulation. It is therefore of great importance to characterize the stimulated fracture network and understand flow patterns in the fracture network before heat production. Many techniques have been employed to monitor the development of hydraulic fractures and characterize the hydraulic connectivity of fracture networks, including electrical resistivity tomography (ERT), seismic imaging, distributed acoustic sensing (DAS), distributed temperature sensing (DTS) and tracer test (Fischer, et al., 2008; Ayling et al., 2016; Knox et al., 2016; Chen et al., 2018; Gao et al., 2018; Mattson et al., 2018; Wu et al., 2018). Among these techniques, tracer test has proven to be an effective method for identifying flow patterns, such as preferential flow channels, in unconventional reservoirs (Dverstorp et al., 1992; Guo et al., 2016b; Zhou et al., 2018).

EGS Collab project is an ongoing *in situ* experiment designed to investigate the stimulation of fracture networks in rocks and circulation of fluids in these fracture networks at an intermediate scale (between the laboratory bench scale and field scales), coupled with geophysical

[4] J. Ajo-Franklin, S.J. Bauer, T. Baumgartner, K. Beckers, D. Blankenship, A. Bonneville, L. Boyd, S.T. Brown, J.A. Burghardt, T. Chen, Y. Chen, K. Condon, P.J. Cook, P.F. Dobson, T. Doe, C.A. Doughty, D. Elsworth, J. Feldman, A. Foris, L.P. Frash, Z. Frone, P. Fu, K. Gao, A. Ghassemi, H. Gudmundsdottir, Y. Guglielmi, G. Guthrie, B. Haimson, A. Hawkins, J. Heise, C.G. Herrick, M. Horn, R.N. Horne, J. Horner, M. Hu, H. Huang, L. Huang, K. Im, M. Ingraham, T.C. Johnson, B. Johnston, S. Karra, K. Kim, D.K. King, T. Kneafsey, H. Knox, J. Knox, D. Kumar, K. Kutun, M. Lee, K. Li, R. Lopez, M. Maceira, N. Makedonska, C. Marone, E. Mattson, M.W. McClure, J. McLennan, T. McLing, R.J. Mellors, E. Metcalfe, J. Miskimins, J.P. Morris, S. Nakagawa, G. Neupane, G. Newman, A. Nieto, C.M. Oldenburg, W. Pan, R. Pawar, P. Petrov, B. Pietzyk, R. Podgorney, Y. Polsky, S. Porse, S. Richard, B.Q. Roberts, M. Robertson, W. Roggenthen, J. Rutqvist, D. Rynders, H. Santos-Villalobos, M. Schoenball, P. Schwering, V. Sesetty, A. Singh, M.M. Smith, H. Sone, C.E. Strickland, J. Su, C. Ulrich, N. Uzunlar, A. Vachaparampil, C.A. Valladao, W. Vandermeer, G. Vandine, D. Vardiman, V.R. Vermeul, J.L. Wagoner, H.F. Wang, J. Weers, J. White, M.D. White, P. Winterfeld, T. Wood, H. Wu, Y.S. Wu, Y. Wu, Y. Zhang, Y.Q. Zhang, J. Zhou, Q. Zhou, M.D. Zoback

monitoring (optical/acoustic televiewer logging, seismic tomography, and ERT) and hydraulic characterization tests (flow test and tracer test) (Kneafsey et al., 2018; Kneafsey et al., 2019; White et al., 2019). The first testbed of the project is in the West Access Drift of the Sanford Underground Research Facility in South Dakota at 4,850 feet below ground in the Poorman Formation. Eight wells were drilled into the experimental volume (Fig. 1(a)), including an injection well (E1-I), a production well (E1-P), four monitoring wells parallel to the expected hydraulic fracture (PDT, PDB, PST and PSB), and two monitoring wells almost orthogonal to the expected hydraulic fracture (E1-OT and E1-OB). In Experiment 1 of the EGS Collab project, several stimulation activities are performed at different notches along E1-I to create hydraulic fractures to connect E1-I and E1-P. During the stimulation activities, ERT data, seismic events and DTS data are obtained for the subsequent analysis of the location and extents of the stimulated hydraulic fractures. After the stimulation activities, flow test and tracer test are conducted to investigate the hydraulic connectivity of the fracture network (White et al., 2019).

In the present study, we attempt to characterize aperture distributions and flow patterns in the created fracture network in Experiment 1 of the EGS Collab project through the modeling of tracer test. Results from seismic imaging, core logs, DTS and flow measurements are used to develop a fracture model which involves a hydraulic fracture (HF) and a natural fracture (NF). A brute-force, Monte Carlo approach is then employed to run massive realizations to simulate tracer transport processes in the hydraulic and natural fractures by utilizing the flow and tracer transport solvers in GEOS (Guo et al., 2016b). Realizations that yield good agreement between simulated and measured tracer breakthrough curves (BTCs) are selected to analyze aperture distributions and flow patterns in the fracture network.

2. HYDRAULIC STIMULATION AND TRACER TEST

In this study, we focus on the hydraulic stimulation and characterization activities performed at 164' Notch (Fig. 1(a)). The details of the stimulation procedure and characterization tests are described in White et al. (2019). During the stimulation, flow out of E1-P and E1-OT are noted. A pressure decay during the shut-in period is observed, indicating that the stimulated hydraulic fracture may have intersected a natural fracture. In addition, DTS signals are observed at E1-OT and PDT, which means that the hydraulic fracture intersects E1-OT and PDT at the two locations indicated by the DTS signals (Fig. 1(a)). Seismic events are also shown in Fig. 1(a). From these observations, the extent of the hydraulic fracture is estimated as shown in Fig. 1(a), connecting E1-I, E1-OT, E1-P, PDT and PDB. A natural fracture intersecting the hydraulic fracture is also assumed in Fig. 1(a) according to core logs and a sewer camera log of E1-P (White et al., 2019).

To characterize the hydraulic connectivity of the stimulated fracture network, a conservative tracer test was performed on October 31st as shown in Fig. 1(b). The injection rate is 400 ml/min, and 0.64 g tracer are injected with an initial concentration of C_0 = 305 ppm. During the tracer test, flow rates at different monitoring wells are measured as annotated in Fig. 1(b). The mass recovery rate of flow is 74%. Note that E1-P intersects both the hydraulic fracture and the natural fracture. The flow rate at its intersection with the hydraulic fracture (E1-PBottom) is 80 ml/min, and the flow rate at its intersection with the natural fracture (E1-PInterval) is also 80 ml/min. Fluid samples are collected at these monitoring wells for subsequent measurement of tracer concentration. During the 7 hours measurement, tracer signals are detected at E1-PBottom, E1-PInterval and E1-OT, and the BTC at E1-PBottom shows the earliest breakthrough time and the largest relative concentration (Fig. 1(c)). The total mass recovery rate of tracer is only 8%.

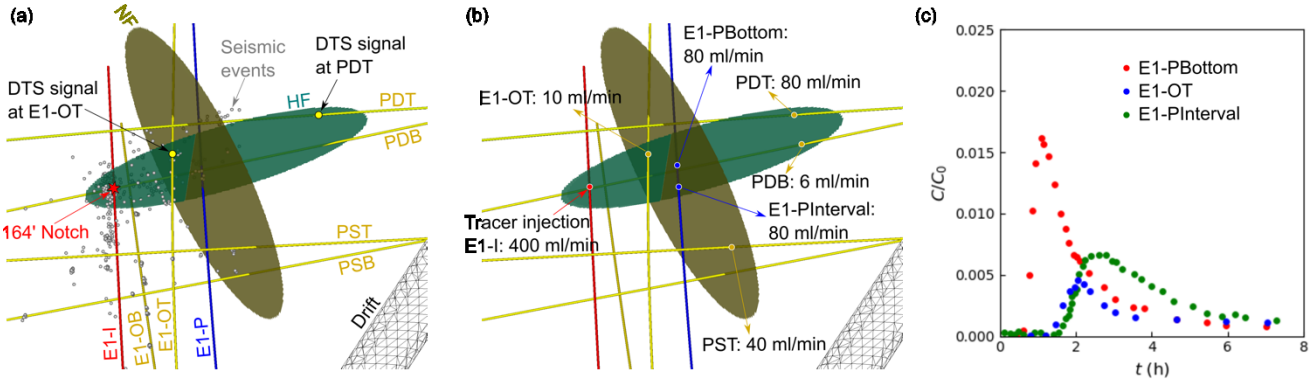

Figure 1: Hydraulic stimulation and tracer test at 164' Notch in Experiment 1 of the EGS Collab project. (a) Configuration of injection, production and monitoring wells. Observed seismicity events and DTS signals during the hydraulic stimulation are shown. Based on these observations as well as core logs, a hydraulic fracture and a natural fracture are estimated and shown. (b) Flow rates at different wells during the tracer test. (c) BTCs at E1-PBottom, E1-OT and E1-PInterval.

3. MODEL AND METHODOLOGY

Based on the above analysis, a fracture model consisting of an elliptical hydraulic fracture and an elliptical natural fracture is developed for tracer modeling (Fig. 2(a)). The matrix is not considered in the fracture model. The two fractures are coupled through a conductive segment (leakage interface) on their intersection. Tracer transport process in the fracture model is then modeled in a sequential manner (Fig. 2(b)). In the first step, we simulate tracer transport in the hydraulic fracture. The location of the leakage interface and the leakage rate from the hydraulic fracture to the natural fracture (q_l) are treated as input parameters in this step. Note that the leakage rate is uniformly distributed along the leakage interface. After the first step, we can obtain the BTCs at E1-PBottom and E1-OT. Time-concentration curves at each element along the leakage interface can also be obtained and then used as boundary conditions in the second step to model tracer transport in the natural fracture and calculate the BTC at E1-PInterval.

Parameters for the fracture model are shown in Fig. 2(c). For the hydraulic fracture, parameters include the two semi-axis lengths A_1 and A_2, aperture w, hydrodynamic dispersion coefficient D_f, location of the leakage interface P_1 and P_2, and leakage rate q_l. Because the flow is not 100% recovered, we also assume a sink on the periphery of the hydraulic fracture to account for flow/tracer leakage from the hydraulic fracture to matrix. Two parameters θ and L are used to describe the location and length of the sink respectively. For the natural fracture, the fracture extent is fixed, and three parameters w', θ' and L' are used for aperture, location and length of the sink on the periphery of the natural fracture respectively. We consider both the uniform aperture scenario and heterogeneous aperture scenario. For uniform aperture scenario, w and w' are two numbers. For heterogeneous aperture scenario, we use spatially correlated aperture distributions for the hydraulic and natural fractures, and w (w') is determined by three parameters, i.e., average aperture $\overline{w}$ ($\overline{w'}$), standard deviation σ (σ') and correlation length CL (CL').

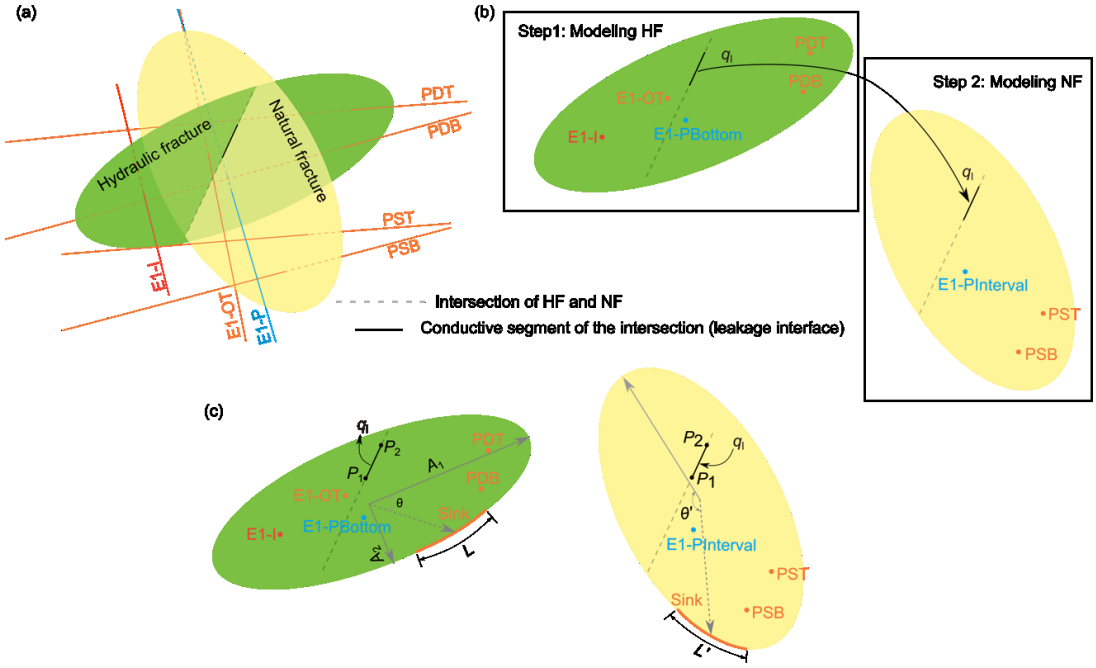

Figure 2: The developed fracture model and simulation strategy for tracer transport in the model. (a) Fracture model consists of a hydraulic fracture and a natural fracture. The two fractures are coupled by a conductive segment of their intersection. (b) Sequential modeling of tracer transport processes in the fracture model. (c) Parameters in the fracture model.

Although data from seismic monitoring, core logs, DTS and flow measurements provides significant information to constrain the fracture model, the system is still under-constrained due to its intrinsic complexity. As mentioned above, there are 12 parameters if we assume uniform aperture distributions in the hydraulic and natural fractures, and 16 parameters if we assume heterogeneous aperture distributions in them. For such a high-dimensional problem, Monte Carlo may be the only feasible method. In addition, for heterogeneous aperture scenario, the aperture field cannot be parameterized using continuous function forms, and some deterministic methods such as Bayesian inversion may not be able to yield desired results (Vogt et al., 2012). Therefore, a brute-force, Monte Carlo approach is employed in this study to simulate tracer transport processes in the fracture model. Massive realizations are performed to obtain viable solutions that yield optimal fits of the measured tracer BTCs in Fig. 1(c).

For each realization, the following workflow is employed: 1) A random parameter set is first generated. The ranges of these parameters are listed in Table 1. Note that the leakage interface is an arbitrary consecutive segment along the intersection of the hydraulic and natural fractures. Also note that the leakage rate q_l needs to satisfy flow rates in both the hydraulic and natural fractures. 2) According to the aperture parameters, a uniform or a heterogeneous aperture field is generated and applied to the hydraulic or natural fracture. 3) The flow solver in GEOS is called to calculate the flow field in the fracture model according to the aperture field with all the flow measurements in Fig. 1(b) being honored. In GEOS model, the fractures are represented by thin layers of porous medium with an equivalent porosity, and the permeabilities of the fractures are calculated according to the cubic law (Guo et al., 2016b). Based on the calculated flow field, the tracer solver with the upwind difference scheme in GEOS is called to calculate tracer transport process in the fracture model. 4) A function is then used to calculate the misfit between the simulated and measured BTCs. For the hydraulic fracture, the function is

$$R_i = \sum_{j=1}^{j=n_{i\_PB}} \left[\left(\frac{p_{i\_PB\_j}}{p_{m\_PB}} - 1 \right)^2 + \left(\frac{t_{i\_PB\_j}}{t_{m\_PB}} - 1 \right)^2 \right] + \sum_{j=1}^{j=n_{i\_OT}} \left[\left(\frac{p_{i\_OT\_j}}{p_{m\_OT}} - 1 \right)^2 + \left(\frac{t_{i\_OT\_j}}{t_{m\_OT}} - 1 \right)^2 \right] \quad (1)$$

where R_i is the misfit for the i_{th} realization; n_{i_PB} and n_{i_OT} are the number of peaks on the simulated BTCs at E1-PBottom and E1-OT respectively (Although the measured tracer BTCs only have one peak, the simulated BTCs may have multiple peaks); $p_{i\_PB\_j}$ and $t_{i\_PB\_j}$, $p_{i\_OT\_j}$ and $t_{i\_OT\_j}$ are the magnitude and time of the j_{th} peak on the simulated BTCs at E1-PBottom and E1-OT respectively; p_{m_PB} and t_{m_PB}, p_{m_OT} and t_{m_OT} are the magnitude and time of the peak on the measured BTCs at E1-PBottom and E1-OT respectively. For the natural fracture, the function is

$$R_i = \sum_{j=1}^{j=n_{i\_PI}} \left[\left(\frac{p_{i\_PI\_j}}{p_{m\_PI}} - 1 \right)^2 + \left(\frac{t_{i\_PI\_j}}{t_{m\_PI}} - 1 \right)^2 \right] \qquad (2)$$

where n_{i_PI} is the number of peaks on the simulated BTC at E1-PInterval; $p_{i\_PI\_j}$ and $t_{i\_PI\_j}$ are the magnitude and time of the j_{th} peak on the simulated BTC at E1-PInterval respectively; p_{m_PI} and t_{m_PI} are the magnitude and time of the peak on the measured BTC at E1-PInterval respectively. To select successful realizations, we sort all the realizations in an ascending order of the calculated misfit. The parameters and aperture distributions of the top realizations are then systematically analyzed to gain insights of the fracture flow patterns.

Table 1: Ranges of parameters for the brute-force, Monte Carlo approach to simulate tracer transport processes in the fracture model.

Uniform aperture scenario						
Parameter	A_1 (m)	A_2 (m)	w (mm)	D_f (m^2/s)	q_l (ml/min)	θ (°)
Range	14 ~ 17	8 ~ 13	0.01 ~ 1	10^{-9} ~ 10^{-6}	120 ~ 224	0 ~ 360
Parameter	L (m)	w' (mm)	θ' (°)	L' (m)		
Range	3 ~ 15	0.05 ~ 10	0 ~ 360	3 ~ 15		
Heterogeneous aperture scenario (additional parameters)						
Parameter	$\overline{w}$ (mm)	σ (mm)	CL (m)	$\overline{w'}$ (mm)	σ' (mm)	CL' (m)
Range	0.01 ~ 0.5	0.01 ~ 0.5	4 ~ 15	0.5 ~ 5	0.5 ~ 5	4 ~ 20

4. RESULTS

4.1 Modeling of tracer transport in the hydraulic fracture with a uniform aperture

As mentioned before, we first model tracer transport in the hydraulic fracture. A uniform aperture is assumed, and about 2,000,000 realizations are performed. Using the misfit function in equation (1), three realizations that yield good fit of the BTCs at E1-PBottom and E1-OT are selected as shown in Fig. 3. The parameters for the three realizations are similar, and an estimation of these parameters are obtained as: A_1 = 16.8 m, A_2 = 11.1 m, w = 0.14 mm, θ = 245°, L = 13 m, q_l = 212 ml/min, and the magnitude of D_f is about 10^{-7} m^2/s. Another commonality is the location of the sink, that all the three realizations indicate a sink to the left of the hydraulic fracture.

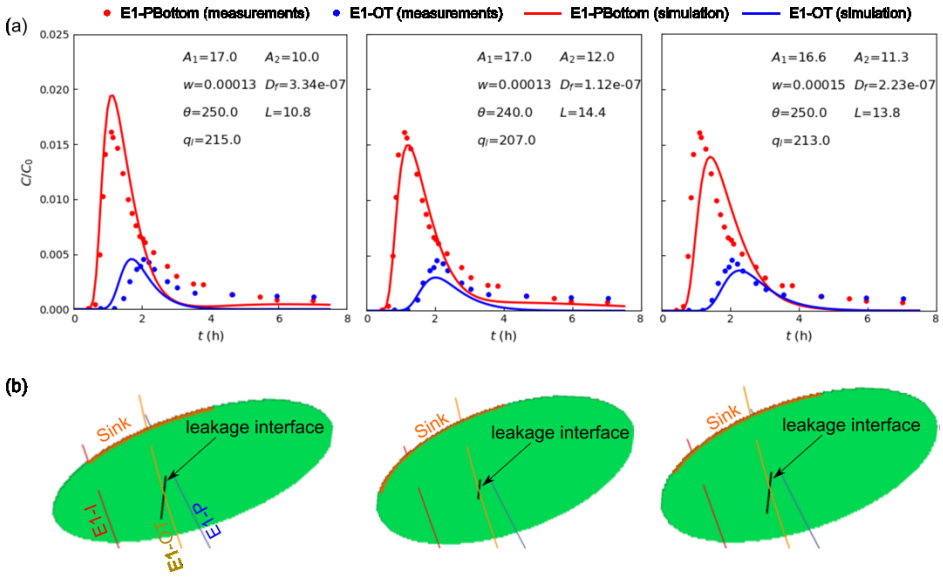

Figure 3: Selected modeling results of tracer transport in the hydraulic fracture with a uniform aperture. (a) Comparison of the BTCs at E1-PBottom and E1-OT for the three realizations. Parameters used in each realization are also annotated. (b) Location and length of the sink and leakage interface for the three realizations.

4.2 Modeling of tracer transport in the natural fracture

We use the results from the first realization in Fig. 3(a) to model tracer transport in the natural fracture. First we assume a uniform aperture in the natural fracture and perform about 800,000 realizations. The selected top fits are shown in Fig. 4(a). The parameters are similar but none of them is able to yield an acceptable goodness of fit for the BTC at E1-PInterval. We then perform another 800,000 realizations assuming a heterogeneous aperture distribution in the natural fracture, and the selected top fits are shown in Fig. 4(b). All of them show

a good match for the BTC at E1-PInterval, but it is difficult to find commonality in parameter values (Fig. 4(b)) and aperture distributions (Fig. 4(c)) among these realizations.

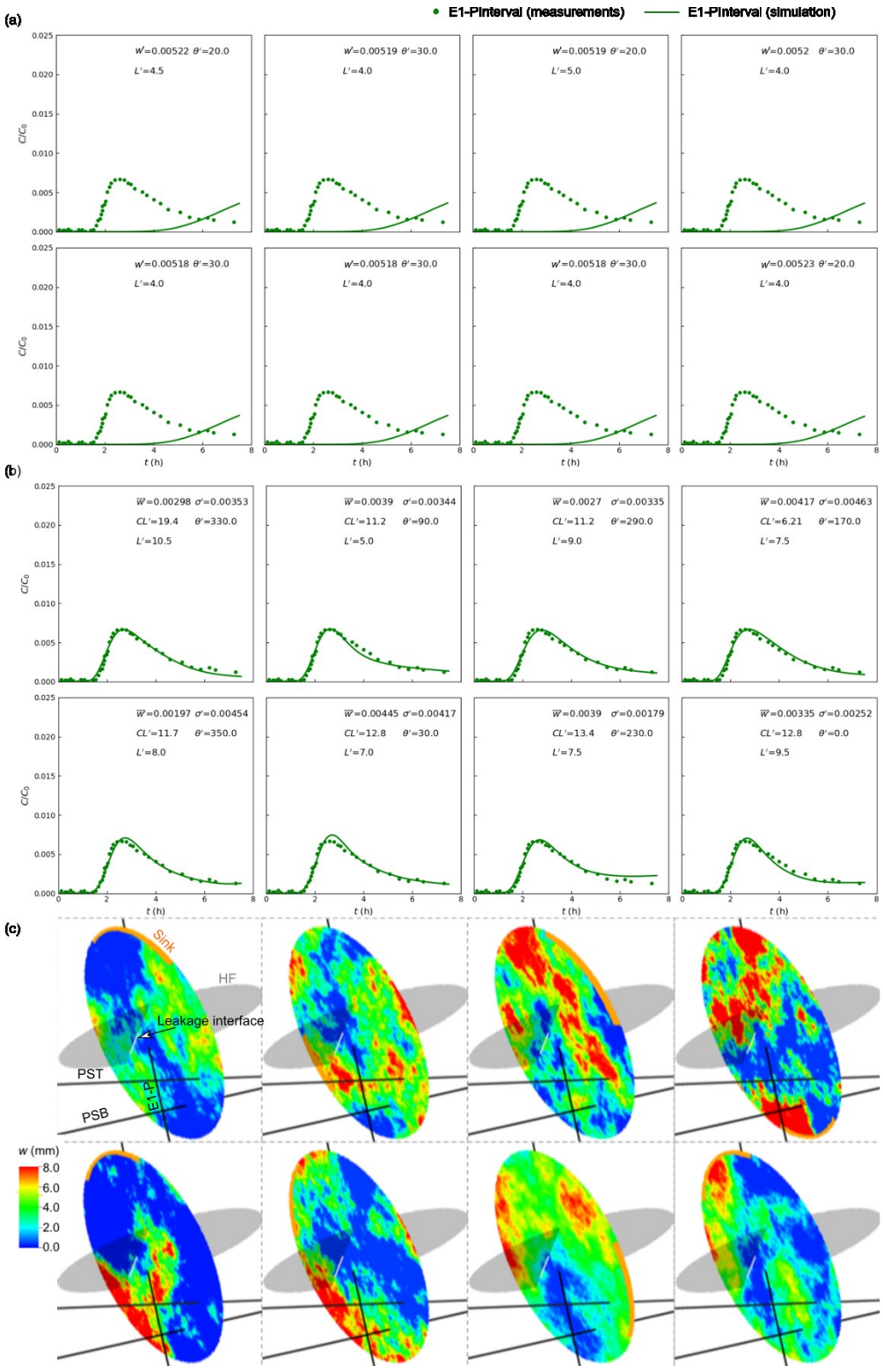

Figure 4: Selected modeling results of tracer transport in the natural fracture. (a) Selected top fits for the uniform aperture scenario. (b) Selected top fits for the heterogeneous aperture scenario. (c) Aperture distributions in the natural fracture corresponding to the realizations in (b).

4.3 Modeling of tracer transport in the hydraulic fracture with a heterogeneous aperture

In this section, we revisit the modeling of tracer transport in the hydraulic fracture by assuming a heterogeneous aperture. About 1,640,000 realizations are performed, and Fig. 5 shows ten of the top fits from these realizations. Fig. 5(b) shows the heterogeneous aperture distributions for the ten realizations, and we cannot identify any common feature in these aperture distributions. One commonality among these realizations is the location of the sink. Similar to the uniform aperture scenario, all the ten realizations in Fig. 5 indicate that the sink locates to the left of the hydraulic fracture.

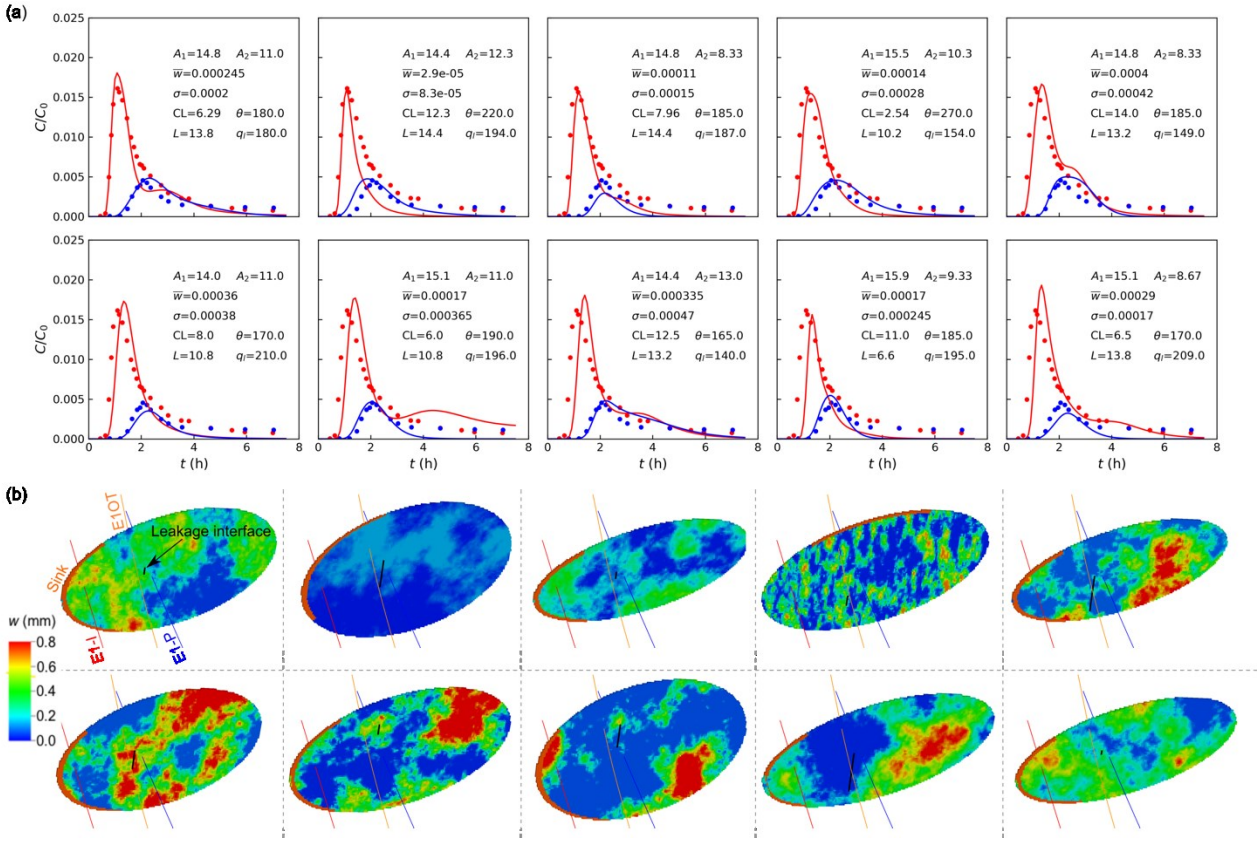

Figure 5: Selected modeling results of tracer transport in the hydraulic fracture with a heterogeneous aperture distribution. (a) Comparison of the BTCs at E1-PBottom and E1-OT. Parameters used in each realization are also annotated. (b) Aperture distribution, as well as location and length of the sink and leakage interface in the selected realizations.

5. CONCLUSIONS

A unified, high-fidelity model incorporating applicable field measurements, including results from seismic imaging, DTS, core logs and flow measurements at different wells, is developed to characterize the fracture flow patterns in Experiment 1 of the EGS Collab project. We use a brute-force, Monte Carlo approach to simulate tracer transport in the model, and multiple solutions that yield optimal fits of the measured tracer breakthrough curves are obtained. By analyzing the commonalities in these solutions, the following conclusions about the aperture distributions and flow patterns in the hydraulic and natural fractures are drawn.

All the obtained solutions indicate that there might be a sink at the left periphery of the hydraulic fracture. During the stimulation activities and tracer test, fluid/tracer may leak from the hydraulic fracture to matrix through this sink. For the hydraulic fracture, both the uniform and heterogeneous aperture scenarios can fit the measured tracer breakthrough curves, while for the natural fracture, a heterogeneous aperture is necessary to fit the measured tracer breakthrough curve. Compared with the flow field in the hydraulic fracture, flow field in the natural fracture might be more channelized. According to the obtained viable solutions, the aperture in the hydraulic fracture is estimated to be about 100 microns, and the aperture in the natural fracture is about one magnitude larger.

Due to the intrinsic complexity of the subsurface fracture system, the problem is still high-dimensional although multiple field measurements have been used to constrain the model. For such an under-constrained problem, we are unable to obtain deterministic patterns of the heterogeneous aperture distributions in hydraulic and natural fractures. It is therefore beneficial to further constrain the model using results from other geophysical tests, including ERT and future tracer tests involving both conservative and non-conservative tracers.

ACKNOWLEDGEMENT

This material was based upon work supported by the U.S. Department of Energy, Office of Energy Efficiency and Renewable Energy (EERE), Office of Technology Development, Geothermal Technologies Office, under Award Number DE-AC52-07NA27344.

Publication releases for this manuscript are under LLNL-CONF-767033. The United States Government retains, and the publisher, by accepting the article for publication, acknowledges that the United States Government retains a non-exclusive, paid-up, irrevocable, world-wide license to publish or reproduce the published form of this manuscript, or allow others to do so, for United States Government purposes. The research supporting this work took place in whole or in part at the Sanford Underground Research Facility in Lead, South Dakota. The assistance of the Sanford Underground Research Facility and its personnel in providing physical access and general logistical and technical support is acknowledged.

REFERENCES

Ayling, B.F., Hogarth, R.A., Rose, P.E.: Tracer testing at the Habanero EGS site, central Australia, *Geothermics*, **63**, (2016), 15-26.

Brown, D.W., Duchane, D.V., Heiken, G., Hriscu, V.T.: Mining the earth's heat: Hot dry rock geothermal energy, Springer-Verlag (2012).

Chen, Y., Huang, L., Ajo-Franklin, J., Kneafsey, T.J., Team, E.C.: Toward real-time microearthquake event detection and location in anisotropic media using a multiscale approach for EGS Collab experiments, Geothermal Resources Council 2018 Annual Meeting Geothermal Resources Council Transactions, Reno, NV (2018).

Cladouhos, T.T., Petty, S., Swyer, M.W., Uddenberg, M.E.: Results from Newberry Volcano EGS Demonstration, 2010-2014, *Geothermics*, **63**, (2016), 44-61.

Dverstorp, B., Andersson, J., Nordqvist, W.: Discrete fracture network interpretation of field tracer migration in sparsely fractured rock, *Water Resource Research*, **28**, (1992), 2327-2343.

Fischer, T., Hainzl, S., Eisner, L., Shapiro, S.A., Le Calvez, J.: Microseismic hydraulic fracture imaging: The path toward optimizing shale gas production, *Journal of Geophysical Research B: Solid Earth*, **113**, (2008), B02307.

Fu, P.C., Hao, Y., Walsh, S.D.C., Carrigan, C.R.: Thermal drawdown-induced flow channeling in fractured geothermal reservoirs, *Rock Mechanics and Rock Engineering*, **49**, (2016), 1001-1024.

Gao, K., Huang, L., Chi, B., Ajo-Franklin, J., Team, E.C.: Imaging the fracture zone using continuous active source seismic monitoring for the EGS Collab project: A synthetic study, 43rd Workshop on Geothermal Reservoir Engineering, Stanford University, Stanford, California (2018).

Guo, B., Fu, P.C., Hao, Y., Peters, C.A., Carrigan, C.R.: Thermal drawdown-induced flow channeling in a single fracture in EGS, *Geothermics*, **61**, (2016a), 46-62.

Guo, B., Fu, P.C., Hao, Y., Carrigan, C.R.: Investigating the possibility of using tracer tests for early identification of EGS reservoirs prone to flow channeling, 41st Stanford Geothermal Workshop, Stanford University, Stanford, CA (2016b).

Kneafsey, T.J., Dobson, P., Blankenship, D., Morris, J., Knox, H., Schwering, P., White, M., Doe, T., Roggenthen, W., Mattson, E., Podgorney, R., Johnson, T., Ajo-Franklin, J., Valladao, C., Team, E.C.: An overview of the EGS Collab project: Field validation of coupled process modeling of fracturing and fluid flow at the Sanford Underground Research Facility, Lead, 43rd Workshop on Geothermal Reservoir Engineering, Stanford University, Stanford, California (2018).

Kneafsey, T.J., Blankenship, D., Knox, H.A., Johnson, T.C., Ajo-Franklin, J.B., Schwering, P.C., Dobson, P.F., Morris, J.P., White, M.D., Podgorney, R., Roggenthen, W., Doe, T., EGS Collab Team: EGS Collab project: Status and progress, 44th Stanford Geothermal Workshop, Stanford University, Stanford, CA (2019).

Knox, H.A., Ajo-Franklin, J.B., Johnson, T.C., Morris, J.P., Grubelich, M.C., Preston, L.A., Knox, J.M., King, D.K.: Imaging fracture networks using joint seismic and electrical change detection techniques, 50th US Rock Mechanics Geomechanics Symposium, Houston, Texas (2016).

Lu, S.M.: A global review of enhanced geothermal system (EGS), *Renewable and Sustainable Energy Reviews*, **81**, (2018), 2902-2921.

Mattson, E., White, M., Zhang, Y., Johnston, B., Hawkins, A., Team, E.C.: Fracture characterization: Preliminary results from the modeling and flow testing of experiment 1, Geothermal Resources Council 2018 Annual Meeting Geothermal Resources Council Transactions, Reno, NV (2018).

McClure, M., Horne, R.N.: An investigation of stimulation mechanisms in Enhanced Geothermal Systems, *International Journal of Rock Mechanics & Mining Sciences*, **72**, (2014), 242-260.

Vogt, C., Kosack, C., Marquart G.: Stochastic inversion of the tracer experiment of the enhanced geothermal system demonstration reservoir in Soultz-sous-Forêts — Revealing pathways and estimating permeability distribution, *Geothermics*, **42**, (2012), 1-12.

White, M.D., Johnson, T.C., Fu, P.C., Wu, H., Ghassemi, A., Lu, J.R., Huang, H., Neupane, H., Oldenburg, C., Doughty, C., Johnson, B., Winterfeld, P., Pollyea, R., Jayne, R., Hawkins, A., Zhang, Y.R., EGS Collab Team: The necessity for iteration in the application of numerical simulation to EGS: Examples from the EGS Collab test bed 1, 44th Stanford Geothermal Workshop, Stanford University, Stanford, CA (2019).

Wu, H., Fu, P.C., Yang, X.J., Morris, J.P., EGS Collab Team: Imaging hydraulic fracture extents and aperture using electrical resistivity tomography, 43rd Workshop on Geothermal Reservoir Engineering, Stanford University, Stanford, CA (2018).

Zhou, Q., Oldenburg, C.M., Kneafsey, T.J., Team, E.C.: Modeling transport of multiple tracers in hydraulic fractures at the EGS Collab test site, 43rd Workshop on Geothermal Reservoir Engineering, Stanford University, Stanford, California (2018).